

Dissecting Streptavidin-Biotin Interaction with a Laminar Flow Chamber

Anne Pierres, Dominique Touchard, Anne-Marie Benoliel, and Pierre Bongrand

Laboratoire d'Immunologie, INSERM U 387, Hôpital Ste-Marguerite, BP 29, 13274 Marseille Cedex 09, France

ABSTRACT A laminar flow chamber was used to study single molecule interactions between biotinylated surfaces and streptavidin-coated spheres subjected to a hydrodynamic drag lower than a piconewton. Spheres were tracked with 20 ms and 40 nm resolution. They displayed multiple arrests lasting between a few tens of milliseconds and several minutes or more. Analysis of about 500,000 positions revealed that streptavidin-biotin interaction was multiphasic: transient bound states displayed a rupture frequency of 5.3 s^{-1} and a rate of transition toward a more stable configuration of 1.3 s^{-1} . These parameters did not display any significant change when the force exerted on bonds varied between 3.5 and 11 pN. However, the apparent rate of streptavidin-biotin association exhibited about 10-fold decrease when the wall shear rate was increased from 7 to 22 s^{-1} , which supports the existence of an energy barrier opposing the formation of the transient binding state. It is concluded that a laminar flow chamber can yield new and useful information on the formation of molecular bonds, and especially on the structure of the external part of the energy landscape of ligand-receptor complexes.

INTRODUCTION

A major property of biomolecules is to bind a variety of ligands in order to fulfill a specific function such as mediating cell adhesion, triggering receptor-mediated cell activation or regulating intracellular networks. During the last decades, it became clear that simple parameters such as affinity or kinetic association and dissociation constants did not fully account for the binding behavior of cell receptors (Bell, 1978). Thus, the capture of flowing leukocytes by activated endothelium probably requires molecular associations endowed with especially high mechanical strength (Lawrence and Springer, 1991). The uptake of soluble ligands by surface-bound molecules is probably dependent on molecular length and flexibility (Pierres et al., 1998a). The recognition by T lymphocytes of complexes formed between major histocompatibility complex molecules and antigenic peptides may be influenced by transient conformational changes of these complexes (Anderson and McConnell, 1999).

Recently, much new information was obtained on ligand-receptor interaction by monitoring the rupture of single molecular bonds subjected to controlled disruptive forces generated by hydrodynamic flow (Tha et al., 1986; Kaplan-ski et al., 1993; Alon et al., 1995), soft vesicles (Evans et al., 1991, 1994, 2001; Merkel et al., 1999), atomic force microscopy (Florin et al., 1994; Lee et al., 1994; Hinterdorfer et al., 1996; Fritz et al., 1998; Baumgartner et al., 2000), other microcantilever-based devices (Tees et al., 2001), or optical traps (Kuo and Sheetz, 1993; Stout, 2001).

The earlier papers reported experimental determination of bond lifetime, measured on bonds subjected to supposedly constant disruptive forces (Kaplanski et al., 1993; Alon et al., 1995), or unbinding force, i.e., force exerted at the moment of rupture on bonds subjected to increasing distractive stress. Most results could be accounted by a simple formula suggested by George Bell (Bell, 1978; Chen and Springer, 2001):

$$k_{\text{off}}(F) = k_{\text{off}}(0) \cdot \exp(xF/k_{\text{B}}T) \quad (1)$$

where $k_{\text{off}}(F)$ is the dissociation rate (in s^{-1}) of a bond subjected to a distractive force F , k_{B} is Boltzmann's constant and T the absolute temperature. Parameter x was suggested to represent the interaction range, with a dimension of a length.

However, this simple framework rapidly appeared insufficient. First, an experimental study of antigen/antibody interaction suggested that ligand receptor association involved a transient intermediate step with a lifetime of the order of a second (Pierres et al., 1995), which seemed a reasonable concept in view of previous reports (Beeson and McConnell, 1994). Second, it was rapidly found that experimental unbinding forces determined on a given ligand-receptor couple were highly dependent on the time dependence of applied distractive force. Thus, the unbinding force of the avidin-biotin couple decreased from 160 pN (Florin et al., 1994) to about 50 pN (Merkel et al., 1995) when the rate of force increase (i.e., loading rate) was decreased from more than 10,000 pN/s (as used in atomic force microscopy studies) to about 100 pN/s. This point was clarified by Evans and colleagues (Evans and Ritchie, 1997; Evans, 1998) who extended Bell's framework by developing Kramers' theory (Kramers, 1940) of the rate of escape of a Brownian particle from a potential well in viscous medium. They hypothesized that the separation of a ligand from a receptor under force followed a unidimensional path, with an energy-distance curve, determined by the so-called energy landscape,

Submitted September 10, 2001, and accepted for publication March 6, 2002.

Address reprint requests to Pr. Pierre Bongrand, Laboratoire d'Immunologie, INSERM U. 387, Hôpital Ste-Marguerite, BP 29, 13274 Marseille Cedex 09, France. Tel.: 33-491-26-03-31; Fax: 33-491-75-73-28; E-mail: bongrand@marseille.inserm.fr.

© 2002 by the Biophysical Society

0006-3495/02/06/3214/10 \$2.00

displaying sequential maxima, or barriers. They showed that the plot of unbinding force versus the logarithm of the loading rate was composed of sequential straight segments the slope of which might be written as $k_B T/x_i$, where x_i represented the distance between the location of the energy minimum and the i th barrier on the energy landscape (Evans, 1998, 2001). Further, by varying the loading rate on an enormous range of 6 orders of magnitude (from 1 to 10^6 pN/s), these authors were able to detect two barriers on the avidin/biotin energy landscape, with sequential positions at 0.12 nm and 0.5 nm from the energy minimum (Merkel et al., 1999).

In addition to the interest of these experimental approaches to understand the biological function of receptors and ligands, these studies provided an unique opportunity to enhance our understanding of protein structure/function relationship. Indeed, it may be hoped that experimental curves will be compared to results from molecular dynamic simulations, when higher computer power or improved algorithms allow sufficient increase of the timescale of simulated experiments (Grubmüller et al., 1996; Izrailev et al., 1997; Evans, 2001; Isralewitz et al., 2001). Further, it is now possible to analyze the effects of well-defined molecular mutations (Yuan et al., 2000) or environmental changes (Evans et al., 2001) on energy landscapes.

The aim of the present work was to show that the laminar flow chamber operated at low shear rate can provide additional information on the fine properties of ligand-receptor association. We used the streptavidin-biotin interaction as a suitable model in view of the availability of accurate structural data (Weber et al., 1989; Hendrickson et al., 1989; Sano and Cantor, 1995) as well as previous studies of single bond behavior (Merkel et al., 1995, 1999; Florin et al., 1994; Lee et al., 1994; Grubmüller et al., 1996; Izrailev et al., 1997). We studied the motion of streptavidin-coated microbeads along biotin-derivatized surfaces under flow with low shear rate ($7\text{--}22\text{ s}^{-1}$). These spheres exhibited arrests of widely varying duration (from 20 ms to several tens of seconds as detected with our monitoring apparatus). The estimated tension generated by the hydrodynamic drag on a tether retaining a particle varied between ≈ 3.5 and 11 pN. The initial detachment rate at low binding site concentration was estimated at 5.3 s^{-1} with a transition frequency of 1.3 s^{-1} toward a more stable binding state. When the shear rate was increased 3-fold, the binding rate exhibited 10-fold decrease whereas the detachment rate did not display any significant change, suggesting the existence of a barrier slowing the access to the transient binding step. It is concluded that 1) the transient binding states we detected may be of functional significance; and 2) it was difficult with previously described methods to analyze binding states of millisecond duration in presence of a disruptive force lower than 10 pN, since

a force higher than 20 pN was required to achieve bond rupture within a period of time compatible with laboratory experiments. Preliminary results were presented in a previous communication (Pierres et al., 1998b).

MATERIALS AND METHODS

Molecule and surfaces

Streptavidin-coated beads of 2.8 μm diameter (Dynabeads M280) were supplied by Dynal France (Compiègne). The surface density of streptavidin groups on spheres was about 3460 molecules $\cdot \mu\text{m}^{-2}$. Biotinylated surfaces were prepared with two different procedures.

Molecularly smooth surfaces were obtained by sequentially incubating freshly cleaved mica surfaces (Muskovite mica, Metafix, Montdidier, France) with 1 mM NiCl_2 , then biotinyl-(Gly) $_{12}$ -(His) $_6$ NH $_2$ (custom-synthesized by Neosystem, Strasbourg, France and supplied as trifluoroacetate). The surface density of biotin sites was estimated with two complementary methods. The uptake of Alexa-Fluor 488-conjugated streptavidin(S-11223, Molecular Probes) was measured with confocal microscopy (Pierres et al., 1994). This method allowed reproducible determination of biotin site density down to about 1000 molecules/ μm^2 . Another method was used to assay low site density in order to reduce the uncertainty due to nonspecific streptavidin binding: mica surfaces were treated with fluorescein-(Gly) $_{12}$ -(His) $_6$ NH $_2$ (custom synthesized by Neosystem) and fluorescence was measured with confocal microscopy. The peptide surface density was respectively estimated at 5950, 4450, 1730, 230, 130, and 40 molecules/ μm^2 when the peptide concentration used for mica treatment was 1, 0.1, 10^{-2} , 10^{-3} , 10^{-4} , and 10^{-5} mg/ml, respectively. The coefficient of variation was less than 30% for all concentrations used.

A key point in our experiments was to ensure that bead detachment was due to a rupture of biotin-streptavidin interaction rather than separation of adsorbed biotinylated peptides from mica surfaces. Since the strength of peptide adsorption on mica was not known, additional experiments were performed with a coupling procedure that was expected to provide higher mechanical resistance and was found convenient in previous experiments (Pierres et al., 1996). Briefly, glass coverslips were washed with concentrated sulfuric acid, then rinsed overnight and incubated for 60 min at room temperature with 0.1 mg/ml poly-L-lysine (Sigma, no. P1524, mol wt 388,100). They were then washed three times in pH 7.2 phosphate buffer solution (PBS), then treated 15 min with 2.5% glutaraldehyde in PBS, washed again in deionized water, then PBS, and incubated for 2 h at room temperature in PBS containing various concentrations of biotin-(Gly) $_{12}$ -(Lys) $_6$ -NH $_2$ (provided by Neosystem) and 0.2% bovine serum albumin (fraction V, Sigma, no. A7030). Unreacted aldehyde groups were blocked by incubating coverslips overnight with 0.2 M glycine before binding assays.

Flow chamber

Chambers were assembled as previously described (Pierres et al., 1998c) by applying mica sheets against a custom-made Plexiglas block with a cavity of $0.1 \times 6 \times 20\text{ mm}^3$ bearing a toric gasket (Satim, Evenos, France). The chamber was set on the stage of an inverted microscope (IX, Olympus) bearing a long-distance 40X dry objective (n.a. 0.55) and a CCD camera (SPT-M 108CE, Sony, Japan) connected to a videotimer (VTG33, Mussetta, Marseille) and a videotape recorder for delayed analysis. Typically, 2 ml of bead suspension (3,000,000/ml in PBS supplemented with 0.2% bovine serum albumin) were driven through the chamber with a 5 ml syringe mounted on a syringe holder (Razel, supplied by Bioblock, Illkirch, France). In some cases, the specificity of binding events was checked by

blocking adhesion with 1 mM biotin (pure D biotin, UP10685E, supplied by Interchim, no. 040).

Particle tracking

Videotapes were analyzed with a PCVision + digitizer (Imaging Technology, Bedford, MA, supplied by Imasys, Suresnes, France) mounted on a desk computer equipped with a 80486 processor. Pixel size was 0.23 μm . Custom-made software written in assembly language allowed separation of the interlaced fields forming each image, thus yielding 20-ms time resolution. On each field, the sphere center of gravity was determined with about 40 nm accuracy. Also, the area was calculated to detect artifactual events such as sphere collisions or doublet formation. In a typical experiment, about 100 particle trajectories were recorded, amounting to about 20,000 events, defined as sets of four parameters: x and y coordinates of the projection of the sphere center on the chamber floor, time, and particle area.

Data analysis

Shear rate determination

Due to the deformability of the chamber floor, standard equations from fluid mechanics do not allow accurate derivation of the wall shear rate G from the flow rate and chamber dimensions (Goldman et al., 1967; Pierres et al., 2001). This difficulty was overcome with a previously validated procedure (Pierres et al., 2001) by using plots of the mean particle acceleration versus velocity. Curves are dependent on both the Hamaker constant of interaction between particle and surface and the wall shear rate. In the present experimental system, the Hamaker constant was found negligible and G could be derived from the velocity U° corresponding to zero acceleration with the following formula:

$$G = 1.32U^\circ - 2.7 \quad (\text{where } G \text{ is in } \text{s}^{-1} \text{ and } U^\circ \text{ in } \mu\text{m/s}) \quad (2)$$

The validity of this approach was checked experimentally (Pierres et al., 2001). Eq. 2 is valid when G ranges between about 5 and 20 s^{-1} .

Particle selection

Accurate determination of binding frequencies requires to consider only fully sedimented particles: indeed, when the shear rate is increased, the time available for sedimentation decreases and passage of incompletely sedimented spheres might result in artifactual decrease of experimental binding frequencies. This difficulty was overcome by considering only trajectory segments where the dimensional ratio U/aG (where U is particle velocity, a is the radius, and G is the wall shear rate) is less than 0.85, corresponding to a sphere-to-surface distance lower than about 150 nm (Goldman et al., 1967), which is the order of magnitude of the amplitude of vertical Brownian motion ($k_B T/P$ is 120 nm, where k_B is Boltzmann's constant, T is the absolute temperature, and P is the particle weight minus Archimedes force).

Arrest definition

Due to the fluctuations of particle velocity originating from Brownian motion (Fig. 1), there is no absolute way of detecting receptor-mediated particle arrest with 100% specificity and sensitivity. The most efficient procedure was to use empirical criteria for arrest definition and check the validity of our choice with suitable controls. Thus, a moving particle was considered as arrested at some point when the displacement during the following period of time τ was lower than a threshold distance ξ . An

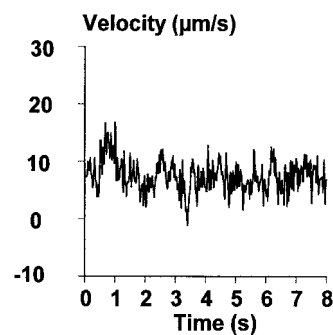


FIGURE 1 Velocity fluctuations of a flowing sphere. The mean velocity of a sphere flowing along a surface was determined for sequential periods of 40 ms (wall shear rate is 7.2 s^{-1}).

arrested particle was considered as resuming its motion when the displacement during the following period of time τ was higher than some threshold $\xi + \Delta$. Introduction of parameter Δ was not essential, but it somewhat improved the efficiency of automatic analysis. A representative arrest is shown on Fig. 2. The relationship between apparent and true arrest duration, i.e., d_a and d_t , can be easily calculated assuming constant velocity for the particle before and after arrest (which is only an approximation). We obtain:

$$d_t = d_a + \tau - (2\xi + \Delta)/v \quad (3)$$

The minimal detectable arrest duration d_m was:

$$d_m = \tau - \xi/v \quad (4)$$

In the present study, particle velocity was studied for three values of the wall shear rate (i.e., about 7, 14, and 21 s^{-1}). The mean ratio U/aG for particles moving with stable velocity along the surface was 0.60 in a pool of 13 separate experiments. Parameters ξ and Δ were set at 1 pixel (0.23 μm) each. Parameter τ was respectively 0.12, 0.08, and 0.04 s when G was 7, 14, and 21 s^{-1} . The shortest detectable arrest durations were thus 0.081, 0.060, and 0.027 s, and the relationship between true and apparent arrest durations were respectively $d_t = d_a + 0.003$ s, $d_t = d_a + 0.021$ s and $d_t = d_a + 0.001$ s.

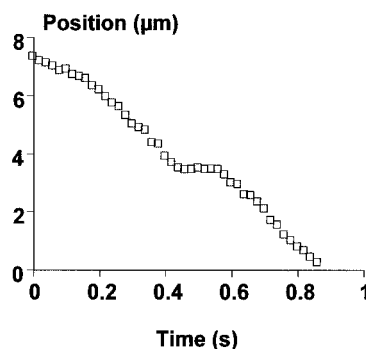


FIGURE 2 Typical arrest. The motion of a streptavidin-coated particle flowing along a biotinylated surface is shown (wall shear rate is 7 s^{-1} , low peptide concentration). A typical arrest appears as a plateau separating two periods of steady motion. The mean velocity during the 160 ms periods before and after arrest are 11.5 $\mu\text{m/s}$ and 9.4 $\mu\text{m/s}$, respectively.

Binding frequency

The binding frequency was obtained by pooling all trajectories in a given experiment and calculating the following ratio:

$$f = \frac{\text{(number of steps followed by an arrest)}}{\text{(number of steps)} \times 50} \quad (5)$$

where a step is defined as an elementary period of time separating two sequential determinations of microsphere position. During data processing, only steps preceded by an arrest-free period of at least 160 ms were counted. This requirement was used to take care of very short displacements with low velocity separating two sequential arrests. Factor 50 is the inverse of step duration (in seconds), allowing to express f in s^{-1} .

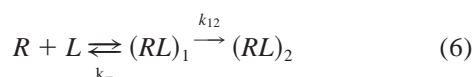
Detachment curves

Arrest durations were used to plot the logarithm of the percentage of particles remaining bound versus time. If arrests were due to single bonds with monophasic behavior, these plots would be straight lines the slope of which would be the negative of the off rate k_{off} . As shown below, experimental curves exhibited marked upward concavity on the time interval [0s, 1s]. Further, the initial slope (corresponding to the first tens of milliseconds) was close to zero. This was an expected artifact, due to the existence of a minimum duration of detectable arrests. Thus, two parameters could be readily extracted from a given curve: 1) the maximum slope or initial detachment rate; a practical way of obtaining this parameter was to calculate the average slope on time interval [0.04, 0.16 s]; 2) the fraction of particles remaining bound 1 s after attachment. Experimental determination was easy since detachment rates at 1 s were fairly low.

Modeling arrest duration

Since results were strongly suggestive of the occurrence of a transient binding step, three parameters were defined: k_- is the rupture frequency of the transient binding step; k_{12} is the frequency of transition from the transient binding step (numbered 1) toward a more stable state (numbered 2) with a lifetime much larger than 1 s.

Thus, the evolution of a single ligand-receptor interaction might be modeled as follows:



These two parameters should allow satisfactory description of the detachment behavior of a bead tethered by a single bond (at low site density). The possibility of multiple bonds was considered by assuming that the number of bonds followed Poisson statistics. However, since receptors and ligands were not expected to display lateral diffusion on beads or surfaces, no bond formation was allowed after the initial contact. Thus, the probability that a particle be bound by i bonds at time 0, provided there was at least one bond, was written as:

$$P_i(0) = [\lambda^i/i!] \exp(-\lambda) / [1 - \exp(-\lambda)] \quad (7)$$

The physical concept underlying this assumption is that adhesion occurs when a sphere approaches the surface to binding distance (as a consequence of Brownian motion) and a bond is formed between a streptavidin molecule located on the sphere, in the contact area, and a biotin group. Poisson parameter λ is thus the product of the number of streptavidin groups in the contact area times the probability of bond formation for a given streptavidin. This parameter is thus expected to be fairly proportional to the biotin site density. Further, a well known property of Poisson law is that the mean number of bond formed during an encounter is equal to λ , and the probability that there is at

least one bond is $[1 - \exp(-\lambda)]$. Thus, the mean number of bonds involved in an attachment event is $\lambda/[1 - \exp(-\lambda)]$.

Defining $P_{i,j}(t)$ as the probability that at time t a particle is tethered by i bonds in weak binding state (1) and j bonds in strong binding state (2), the general equation (for i and j larger than 1) is:

$$\begin{aligned} dP_{i,j}(t)/dt = & k_- [(i+1)P_{i+1,j}(t) - iP_{i,j}(t)] \\ & + k_{12} [(i+1)P_{i+1,j-1}(t) - iP_{i,j}(t)] \quad (8) \end{aligned}$$

Plots of the binding probability $[1 - P_{0,0}(t)]$ versus k_-t were constructed numerically for different values of dimensionless parameters k_{12}/k_- and λ . This was achieved by setting an upper limit to the number of bonds: $i+j \leq 10$, which appeared warranted since experimental data suggested that particle arrests involved a few bonds; indeed, the estimated mean number of bonds was less than 2 for all tested biotin densities.

Statistics

The results obtained in the present paper required to process several thousands of trajectories, yielding 957,732 positions and 1338 arrests. Since it was often necessary to pool the results of several experiments to obtain significant detachment curves, it was important to assess the statistical significance of derived parameters.

Binding frequency was derived from the proportion of time steps followed by an arrest. The theoretical standard deviation was calculated as $(pq/n)^{1/2}$, using well known properties of Poisson distribution. Parameter n is the number of time steps, p is the proportion of steps followed by an arrest and q is $1-p$ (Snedecor and Cochran, 1980).

The standard error on the slope k of a detachment curve between time t_0 and t_1 was obtained by assuming Poisson distribution for the numbers A and B of particles detached respectively at time t between t_0 and t_1 and t_1 and t_0 , respectively. Since k is close to $\ln[B/(A+B)]/(t_1-t_0)$, the standard error may be readily calculated as $[A/B(A+B)]^{1/2}/(t_0-t_1)$.

Force on a bond

The force on a bond maintaining a sphere arrested in presence of a laminar shear flow was calculated with standard mechanical reasoning, assuming no friction at the sphere-to-surface contact and writing that the total force and torque due to the wall, the bond and hydrodynamic forces is zero. Assuming that the bond length L is much smaller than the sphere radius (a) and using published results for the fluid action (Goldman et al., 1967), the tension on the bond may be approximated as $14.3 G a^{5/2} L^{-1/2} \mu$, where G is the shear rate and μ is the medium viscosity. Assuming 5 nm for the bond length, we obtain $T = 0.47G$, where the bond tension T is expressed in piconewtons and G in s^{-1} .

RESULTS

Streptavidin-biotin interaction generates multiple arrests of flowing spheres

In a first series of experiments, spheres were driven with low wall shear rate ($G \approx 7 s^{-1}$) along surfaces pretreated with various concentrations of biotinylated histidine-tagged oligopeptide. As shown in Fig. 3, while controls displayed rare arrests with a frequency of order of $0.1 s^{-1}$, coating surfaces with biotinylated peptides resulted in 5- to 10-fold increase of binding frequency.

When the chamber floor was treated with sequential dilutions of the initial solution, the arrest frequency gradu-

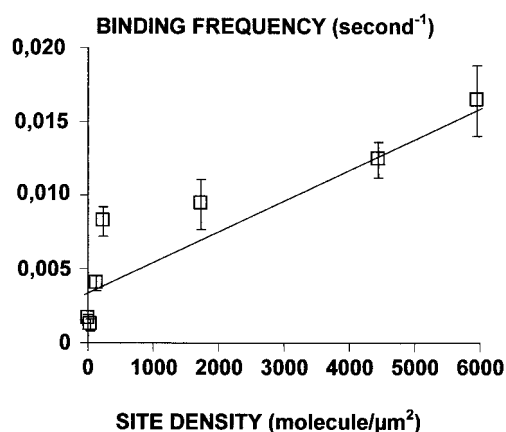


FIGURE 3 Dependence of adhesion frequency on ligand density. Streptavidin-coated spheres were driven along surfaces derivatized with varying densities of biotinylated peptide. The adhesion frequency was determined after monitoring a typical number of 20,000 positions. Vertical bar length is twice the statistical standard error. Each point corresponds to 31 to 111 arrests.

ally decreased. No significant difference was found between controls and surfaces treated with 10^{-5} mg/ml peptide, while the 10^{-3} mg/ml solution (233 biotin sites/ μm^2) yielded fivefold higher arrest frequency than controls.

Finally, when an excess of soluble biotin (1mM) was added to block streptavidin groups on the sphere surface, the binding frequency fell to control level (Table 1). These results show that streptavidin-biotin interaction triggered detectable arrests of flowing spheres.

Many interactions between streptavidin- and biotin-coated surfaces are transient

When a preliminary analysis of the present experimental model was performed (Pierres et al., 1998b) to study the distribution of arrest durations with limited time resolution (the test time step τ used for defining arrests was 0.32 s), the initial rate of particle detachment was much lower than reported in a previous study made on the weak interactions

TABLE 1 Soluble biotin inhibits the binding of streptavidin-coated spheres to biotinylated surfaces

Biotin site density (mol/ μm^2)	Arrest frequency (s^{-1})		% inhibition by soluble biotin
	Without 1 mM biotin	With 1 mM biotin	
4450	0.60 ± 0.13	0.09 ± 0.02	86
1730	0.48 ± 0.07	0.06 ± 0.01	89
230	0.35 ± 0.05	0.03 ± 0.01	93

Streptavidin-coated spheres were driven along biotinylated surfaces in standard medium or in medium supplemented with 1 mM biotin. A total number of 125,549 elementary displacements were recorded and 216 arrests were observed. The arrest frequency was calculated as described and results are shown together with % inhibition by biotin (last column).

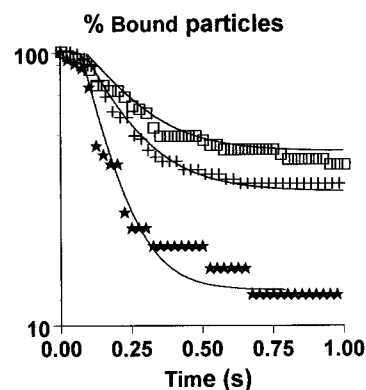


FIGURE 4 Kinetics of particle detachment. Streptavidin-coated spheres were driven along surfaces coated with 5950 molecules/ μm^2 (\square), 233 molecules/ μm^2 (+), or no (*) biotinylated peptide with a wall shear rate of about 7 s^{-1} . The durations of binding events were recorded to build detachment plots. Fitted theoretical curves are also shown (see model described in Methods).

between CD2 and CD48 adhesion molecules (Pierres et al., 1996), which seemed a reasonable finding in view of the high affinity of streptavidin-biotin interaction. However, when the minimum duration of detectable arrests was reduced to about 0.081 s, the analysis of arrest duration revealed the occurrence of many transient interactions. Typical detachment curves are displayed of Fig. 4: when the biotin surface density was high, detachment curves displayed an initial detachment rate of 2.5 s^{-1} with rapid attachment strengthening, since essentially no detachment occurred more than 0.25 s after arrest. When biotin density was decreased, the initial detachment rate fell to about 4 s^{-1} and substantial detachment occurred until 0.5 s after attachment.

Finally, arrests measured on controls displayed still higher maximal detachment rate ($8.8 \pm 1.7 \text{ s}^{-1}$) and only 13% of these arrests lasted more than 1 s, as compared to about 40% of arrests obtained with high biotin density.

The short duration of bead arrests cannot be due to mechanical detachment of adsorbed biotinylated peptides from mica surfaces

A possible interpretation of our results might be that rapid detachment of streptavidin-coated microspheres be due to a rupture of the association between mica and the hexahistidine moiety of biotinylated peptides. In order to rule out this explanation, stronger coupling of biotin to surfaces was performed by covalent coupling of biotinylated peptides to large (388,000 molecular weight) polylysine molecules deposited on glass surfaces. As shown on Table 2, streptavidin-coated beads exhibited transient arrests on these surfaces, and binding frequency was decreased by 86% or more by an excess of soluble biotin (1 mM).

TABLE 2 Observation of transient binding events between streptavidin-coated spheres and glass surfaces derivatized with biotin sites covalently coupled to polylysine molecules

Peptide concentration (mg/ml)	Arrest frequency (s ⁻¹)	Dissociation rate (s ⁻¹)	% inhibition of arrest frequency by soluble biotin
0.1	0.43 ± 0.09	1.27 ± 0.59	86
10 ⁻⁴	0.21 ± 0.03	3.27 ± 0.65	90
10 ⁻⁵	0.24 ± 0.02	3.24 ± 0.56	88
0	0.06 ± 0.02	2.92 ± 1.20	

Streptavidin-coated spheres were driven along glass surfaces coated with polylysine molecules covalently coupled to different amounts of biotinylated peptide. The specificity of sphere-to-surface interaction was checked by adding soluble biotin (1 mM) to block binding events. A total of 384,405 positions were recorded, yielding 271 detectable arrests, binding frequencies and dissociation rates were calculated. Results are shown ± S.D. as described.

Experimental distributions of arrest durations are consistent with the hypothesis that spheres are bound to biotinylated surfaces by a few molecular interactions with an initial rupture frequency of 5.3 s⁻¹ and spontaneous transition toward a more stable binding state with 1.3 s⁻¹ frequency

In view of the known properties of single molecular bonds and the low hydrodynamic drag on flowing spheres (i.e., about 0.5 pN on a sphere and 4 pN on a single bond maintaining the sphere at rest), it seemed reasonable to assume that sphere arrests were due to a few molecular interactions. The maximal detachment rate was determined for sequential peptide dilutions. Results were, respectively: 2.51 ± 0.59 s⁻¹, 2.70 ± 0.46 s⁻¹, 3.98 ± 1.02 s⁻¹, 4.64 ± 0.74 s⁻¹, and 3.77 ± 0.85 s⁻¹ when biotin surface density was respectively 5950, 4450, 1730, 230, and 130 molecules/μm². Since the differences between the last three values were not statistically different, we hypothesized that observed arrests were essentially due to single molecular interactions when the surface density of biotin sites was 1730 molecules/m² or less.

Then, it was attempted to account quantitatively for detachment curves with models involving a minimal number of parameters. We started studying arrest duration on low biotin density surfaces assuming the bond number was 1 at time 0. While it was not feasible to account for experimental data with a standard model (Kaplanski et al., 1993) allowing continuous bond formation and detachment with adjustable rate constants k_+ and k_- (not shown), a very easy fit was obtained with a two-constant biphasic single-bond model assuming a transient intermediate state with detachment rate k_- and transition frequency k_{12} toward a stable bound state. Estimated kinetic parameters were $k_- = 5.26$ s⁻¹ and $k_{12} = 1.32$ s⁻¹, yielding satisfactory agreement with experimental data (Fig. 4).

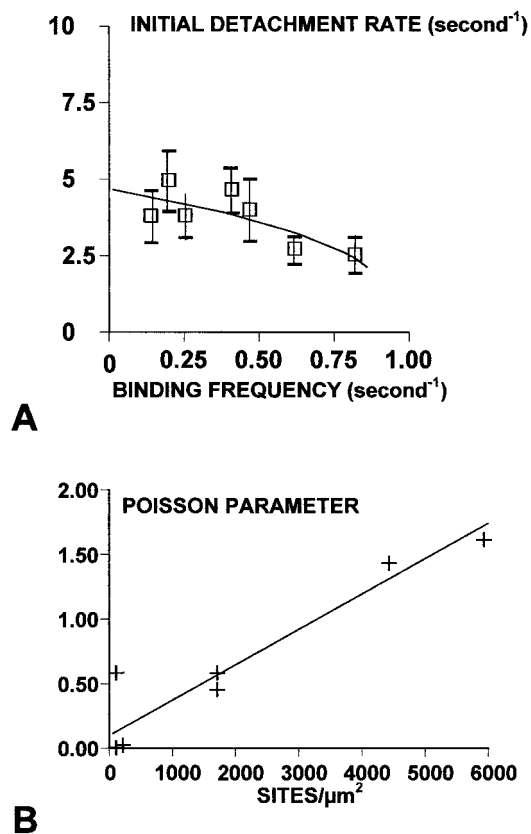


FIGURE 5 Test of Poisson model for bond number. Two independent methods were used to test Poisson model for the bond number distribution. (A) Seven separate sets of experiments were used to determine the frequency of microsphere arrest and initial detachment rate when the biotin site density was varied. Each point represents a numerical result (39 to 111 arrests) and vertical bar length is twice the statistical standard deviation. A theoretical curve was built by varying Poisson parameter λ . For each value of this parameter, initial detachment rate was calculated using previously obtained kinetic constants ($k_- = 5.26$ s⁻¹ and $k_{12} = 1.32$ s⁻¹) and the binding frequency was calculated as $[1 - \exp(-\lambda)] \times 1.004$. The numerical parameter 1.004 was obtained by fitting the experimental value corresponding to the highest binding frequency. (B) The Poisson parameter was derived from the experimental value of the initial detachment rate (using already obtained kinetic constants k_- and k_{12}) and plotted versus biotin site density.

The extension to high biotin densities was achieved by allowing for multiple bonds. We assumed that bond formation during particle to surface contact might be considered as a rare event following Poisson's law. Denoting Poisson parameter as λ , binding frequency should thus be equal to the product of the (unknown) frequency of sphere/surface encounters and $[1 - \exp(-\lambda)]$. Further, the mean bond number after an arrest should be equal to $\lambda/[1 - \exp(-\lambda)]$. As shown in Fig. 5 A, the experimental relationship between attachment frequency and initial detachment rate was satisfactorily accounted for by retaining for k_- and k_{12} the values previously obtained by fitting the curve displayed in Fig. 4 and using for $[1 - \exp(-\lambda)]$ the attachment fre-

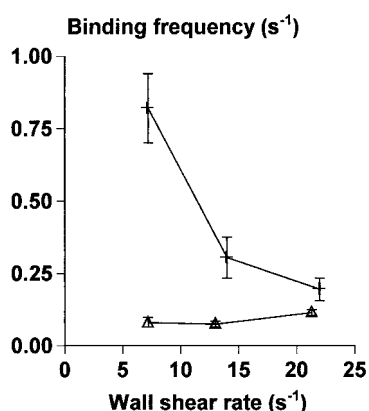


FIGURE 6 Effect of wall shear rate on binding frequency. The dependence of binding frequency on wall shear rate is shown as obtained on controls (Δ) or surfaces coated with 5950 molecules/ μm^2 of biotinylated peptide (+). Vertical bar length is twice the statistical error.

quency (in s^{-1}) times 1.004, as obtained by fitting the theoretical curve and the experimental point corresponding to the highest binding frequency.

A second prediction of the model would be that Poisson parameter λ be proportional to the binding site density when this is low enough. This prediction was tested by deriving λ from the initial detachment rate for different values of the site density. As shown in Fig. 5 B, experimental data were consistent with our model over the entire range of tested biotin surface densities.

Increasing the wall shear rate dramatically decreases the frequency of biotin-mediated attachments without any substantial change of other kinetic parameters

It was interesting to explore the influence of hydrodynamic forces on the formation and dissociation of streptavidin-biotin bonds. As shown in Fig. 6, when the wall shear rate was increased threefold, the frequency of sphere attachment to surfaces coated with high densities of biotin molecules

displayed fourfold decrease whereas the frequency of non-specific (control) attachments increased by 50%. The frequency of specific attachments, defined as the difference between binding frequencies measured on biotin-coated and control surfaces, displayed still more dramatic variations since it decreased from $0.74 \pm 0.13 \text{ s}^{-1}$ to $0.08 \pm 0.004 \text{ s}^{-1}$ when the wall shear rate was increased from 7.2 to 21.8 s^{-1} . As shown in Table 3, detachment rates did not display any significant dependence on the wall shear rate in the studied range.

DISCUSSION

The purpose of this work was to show that the laminar flow chamber operated under low shear rate may be a useful complement to atomic force microscopy (Florin et al., 1994; Lee et al., 1994; Hinterdorfer et al., 1996; Fritz et al., 1998), or biomembrane force probe methodology (Evans et al., 1994, 2001; Merkel et al., 1999) to dissect molecular interactions at the single bond level in order to obtain information on energy landscapes. Four specific features of our method can be emphasized. 1) Since spheres scan a fairly extended area, it is possible to explore surfaces coated with low receptor density. 2) Ligand-receptor contacts are very brief; indeed, the relative velocity between sphere and chamber surfaces is about half the sphere velocity (Goldman et al., 1967), i.e., about $3 \mu\text{m/s}$ for the lowest wall shear rate we used. The contact time for a molecular couple of 3 nm total length borne by interacting surfaces would thus be of order of 1 ms. It is thus possible to analyze transient association states before transition toward the minimum energy level makes the bond resistant to hydrodynamic forces. 3) The force acting on receptors at the moment of rupture ranged between 3.5 and 11 pN. Assuming that this force was low enough to prevent any deformation of interacting surfaces, the loading rate is expected to be higher than about 3500 pN/s (i.e., 3.5 pN/1 ms). Since the loading time is much lower than the arrest duration, bond rupture is thus expected to occur under constant load. This regime is quite different from atomic force microscopy, and

TABLE 3 Effect of wall shear rate on detachment kinetics

Biotin surface density ($\text{mol}/\mu\text{m}^2$)	Wall shear rate			
	7 s^{-1}		22 s^{-1}	
	Initial detachment rate (s^{-1})	Fraction of attached spheres remaining bound 1 s after arrest	Initial detachment rate (s^{-1})	Fraction of attached spheres remaining bound 1 s after arrest
5950	$2.51 \pm 0.59 \text{ s}^{-1}$	39 ± 6.4	$3.64 \pm 1.17 \text{ s}^{-1}$	57 ± 10
230	$4.64 \pm 0.74 \text{ s}^{-1}$	33 ± 5.4	$6.36 \pm 1.23 \text{ s}^{-1}$	21 ± 5.6
0 (control)	$8.77 \pm 1.7 \text{ s}^{-1}$	13 ± 6	$9.98 \pm 1.14 \text{ s}^{-1}$	7.7 ± 2.2

Streptavidin-coated spheres were driven along mica surfaces coated with high (5954 sites/ μm^2) or low (233 sites/ μm^2) densities of biotin groups. Untreated surfaces were also used as controls. The wall shear rate was 7 s^{-1} or 22 s^{-1} . The durations of particle arrests were recorded for determination of initial detachment rate, estimated on time interval [0.03, 0.16 s] and fraction of particle remaining bound 1 s after stopping. Results are shown \pm S.E.M. According to Student's *t*-test, parameters obtained for a given peptide concentration did not exhibit any significant change when the wall shear rate was increased.

theoretical analysis is much simpler. Indeed, the dependence of unbinding force on loading rate is by no means straightforward (Evans and Ritchie, 1997). 4) It is possible to detect bonds with a lifetime of a few tens of milliseconds. Thus, the laminar flow chamber operated under low shear rate is ideally suited to explore weak bonds, or the outer part of the energy landscape of strong ligand-receptor pairs.

The power of this approach is exemplified by our analysis of streptavidin-biotin interaction. Two pieces of information were obtained. 1) Results disclosed the existence of an intermediate binding state with an off rate k_- of 5.26 s^{-1} and a transition frequency toward a stable state $k_{12} = 1.32 \text{ s}^{-1}$. The natural lifetime of this intermediate state was thus $1/(k_- + k_{12}) = 0.15 \text{ s}$. Note that the reality of transient streptavidin-biotin interaction is rigorously demonstrated by the findings that more than 50% of microsphere attachments to biotinylated surfaces lasted less than 1 s, and more than 85% of these attachments were blocked by an excess of soluble biotin (Fig. 4 and Table 1). 2) The dramatic decrease of the binding frequency when the velocity was increased was indicative of a barrier external to the aforementioned transient state. This is in line with a recent report from Chen and Springer (2001) who concluded that the formation of selectin receptor-ligand bond under flow was limited by shear rate whereas dissociation was dependent on applied force. However, the comparison between both sets of results may not be warranted, since cells and model particles may behave quite differently. Our results are also in line with the report that the binding of fibrinogen to a silica surface required a minimal contact time ranging between 50 and 200 ms (Hemmerlé et al., 1999). Our results would be consistent with the occurrence of a very shallow energy minimum outside the detected binding state, leading to a transient state with a lifetime too short to be detected. According to Bell's Eq. 1, a 9.25-fold decrease of the binding frequency (i.e., from 0.74 to 0.08 s^{-1}) when the applied force is increased from 3.4 to 10.3 pN (corresponding to a rise of the wall shear rate from 7.2 to 22 s^{-1}) would be accounted for by a distance of 1.3 nm between the intermediate state and neighboring energy barrier (Fig. 7). It is unlikely that these states be related to the 0.12 and 0.5 nm barriers reported by Merkel et al. (1999) in their study of the streptavidin-biotin interaction: indeed, with a loading rate of 1 pN/s , the mean rupture strength of the streptavidin-biotin bond was about 20 pN , yielding a bond lifetime of 20 s (see Fig. 3 of Merkel et al., 1999). This does not match the 0.15-s lifetime we obtained for state 1 (our Fig. 7) when subjected to a distractive force of about 3.5 pN . However, our findings are consistent with computer simulations from Izrailev et al. (1997); see Fig. 4 of Merkel et al., (1999) suggesting the existence of energy barriers external to the 0.5-nm maximum in the streptavidin-biotin energy landscape. Clearly, complete determination of the energy/distance plot for the streptavidin-biotin complex requires further experimental studies.

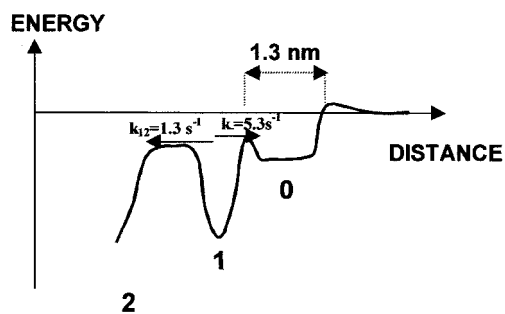


FIGURE 7 Information obtained on streptavidin-biotin interaction. Presented results are consistent with the following scheme. Initial streptavidin-biotin encounter may generate a low stability complex (0) of millisecond or less natural lifetime that cannot be detected. The frequency of complex 0 formation is independent of the shear rate since the decrease of molecular contact duration resulting from velocity increase is compensated by an increase of the frequency of molecular encounters. The complex may shift to a more stable binding state (1) with a frequency that is dependent on the applied force, following Bell's equation. State 1 may undergo spontaneous transition to more stable states (collectively labeled 2) or revert to state 0.

It must be emphasized that the “long distance” part of energy landscapes of surface-bound ligand-receptor complexes may be more dependent on cell surface features unrelated to the intrinsic properties of these ligands and receptors. It would thus be warranted to study more thoroughly the dependence of our data on the method used to couple binding sites on surfaces.

Another point of interest is the information we obtained on nonspecific interactions. Indeed, nonspecific associations are involved in any actual experimental model, and although they are usually minimized to study more useful parameters, it might be warranted to subject them to deeper analysis.

An obvious question is to assess the interest of dissecting ligand-receptor interaction. Transient binding states may influence the initial steps of receptor function. Thus, the ability of a selectin to capture flowing cells is limited by kinetic as well as mechanical properties (Chen and Springer, 2001). Transient binding states may be still more important under conditions of lower mechanical stress than in blood vessels. Thus, the uptake of an antibody-coated bacterium subjected to Brownian motion when encountering a phagocyte requires that the cell receptor bind its ligand within a fraction of a second.

Three points must be considered to assess the validity of our conclusions. First, there is a remote possibility that sphere detachment might involve the rupture of peptide-mica interaction rather than avidin-biotin. However, this is unlikely for three reasons. 1) Since peptide attachment was stable for hours, this should not be so weak as to be unable to resist a force of a few piconewtons for less than a second. 2) The marked bond strengthening we observed within a fraction of a second following attachment was more likely to affect a newly formed association than an attachment

formed several hours before. 3) Transient binding events were readily detected when biotin sites were covalently coupled to large polylysine molecules that were expected to bind to glass surface through multiple electrostatic bonds.

Second, our theoretical model assuming initial formation of multiple bonds and excluding delayed bond formation is especially suited to artificial spheres where no lateral diffusion of surface molecules is expected. This property and the very short length of binding molecules is consistent with the low bond number found even with the highest biotin concentration. Indeed, assuming a ligand + receptor length L of order of 3 nm, the contact area $2\pi aL$ is about $0.026 \mu\text{m}^2$, which would allow the formation of many bonds if binding sites were connected to surfaces through long and flexible linkers.

Third, although it is difficult to estimate the size of ligand-receptor couples with high accuracy, the resulting uncertainty on the force applied to bonds formed between spheres and surfaces is expected to remain low. Indeed, this force is proportional to the square root of (a/L) .

We conclude that the laminar flow chamber operated under low shear rate may provide new and useful information on the fine properties of ligand-receptor bonds.

This work was supported in part by a ministerial grant (Bioinformatics Programme).

REFERENCES

- Alon, R., D. A. Hammer, and T. A. Springer 1995. Lifetime of P-selectin-carbohydrate bond and its response to tensile force in hydrodynamic flow. *Nature*. 374: 539–542.
- Anderson, T. G., and H. M. McConnell. 1999. Interpretation of biphasic dissociation kinetics for isomeric class II major histocompatibility complex-peptide complexes. *Biophys. J.* 77:2451–2461.
- Baumgartner, W., P. Hinterdorfer, W. Ness, A. Raab, D. Vestweber, H. Schindler, and D. Drenthahn. 2000. Cadherin interaction probed by atomic force microscopy. *Proc. Natl. Acad. Sci. U.S.A.* 97:4005–4010.
- Beeson, C., and H. M. McConnell. 1994. Kinetic intermediates in the reactions between peptides and proteins of major histocompatibility complex class II. *Proc. Natl. Acad. Sci. U.S.A.* 91:8842–8845.
- Bell, G. I. 1978. Models for the specific adhesion of cells to cells. *Science*. 200:618–627.
- Chen, S., and T. A. Springer. 2001. Selectin receptor-ligand bonds: formation limited by shear rate and dissociation governed by the Bell model. *Proc. Natl. Acad. Sci. U.S.A.* 98:950–955.
- Evans, E. 1998. Energy landscapes of biomolecular adhesion and receptor anchoring at interfaces explored with dynamic force spectroscopy. *Faraday Discuss.* 111:1–16.
- Evans, E. 2001. Probing the relation between force-lifetime and chemistry in single molecular bonds. *Annu. Rev. Biophys. Biomol. Struct.* 30: 105–128.
- Evans, E., D. Berk, and A. Leung. 1991. Detachment of agglutinin-bonded red blood cells. I. Forces to rupture molecular-point attachments. *Biophys. J.* 59:838–848.
- Evans, E., A. Leung, D. Hammer, and S. Simon. 2001. Chemically distinct transition states govern rapid dissociation of single L-selectin bonds under force. *Proc. Natl. Acad. Sci. U.S.A.* 98:3784–3789.
- Evans, E., R. Merkel, K. Ritchie, S. Tha, and A. Zilker. 1994. Picoforce method to probe submicroscopic actions in biomembrane adhesion. In *Studying Cell Adhesion*. P. Bongrand, P. M. Claesson, and A. S. G. Curtis, editors. Springer Verlag, Heidelberg. 125–139.
- Evans, E., and K. Ritchie. 1997. Dynamic strength of molecular adhesion bonds. *Biophys. J.* 72:1541–1555.
- Florin, E. L., V. T. Moy, and H. E. Gaub. 1994. Adhesion forces between individual ligand-receptor pairs. *Science*. 264:415–417.
- Fritz, J., A. G. Katopodis, F. Kollinger, and D. Anselmetti. 1998. Force-mediated kinetics of single P-selectin/ligand complexes observed by atomic force microscopy. *Proc. Natl. Acad. Sci. U.S.A.* 95:12283–12288.
- Goldman, A. J., R. G. Cox, and H. Brenner. 1967. Slow viscous motion of a sphere parallel to a plane wall. II. Couette flow. *Chem. Eng. Sci.* 22:653–660.
- Grubmüller, H., B. Heymann, and P. Tavan. 1996. Ligand binding: molecular mechanics calculation of the streptavidin-biotin rupture force. *Science*. 271:997–999.
- Hemmerlé, J., S. M. Altmann, M. Maaloum, J. K. H. Hörber, L. Heinrich, J. C. Voegel, and P. Schaaf. 1999. Direct observation of the anchoring process during the adsorption of fibrinogen on a solid surface by force-spectroscopy mode atomic force microscopy. *Proc. Natl. Acad. Sci. U.S.A.* 96:6705–6710.
- Hendrickson, W. A., A. Pähler, J. L. Smith, Y. Satow, E. A. Merritt, and R. P. Phizackerley. 1989. Crystal structure of core streptavidin determined from multi-wavelength anomalous diffraction of synchrotron radiation. *Proc. Natl. Acad. Sci. U.S.A.* 86:2190–2194.
- Hinterdorfer, P., W. Baumgartner, H. J. Gruber, K. Schilcher, and H. Schindler. 1996. Detection and localization of individual antibody-antigen recognition events by atomic force microscopy. *Proc. Natl. Acad. Sci. U.S.A.* 93:3477–3481.
- Israelowitz, B., M. Gao, and K. Schulten. 2001. Steered molecular dynamics and mechanical functions of proteins. *Curr. Opin. Struct. Biol.* 11: 224–230.
- Izrailev, S., S. Stepaniants, M. Balsera, Y. Oono, and K. Schulten. 1997. Molecular dynamics study of unbinding of the avidin-biotin complex. *Biophys. J.* 72:1568–1581.
- Kaplanski, G., C. Farnarier, O. Tissot, A. Pierres, A. M. Benoliel, M. C. Alessi, S. Kaplanski, and P. Bongrand. 1993. Granulocyte-endothelium initial adhesion. Analysis of transient binding events mediated by E-selectin in a laminar shear flow. *Biophys. J.* 64:1922–1933.
- Kramers, H. A. 1940. Brownian motion in a field of force and the diffusion model of chemical reactions. *Physica*. VII: 284–304.
- Kuo, S. C., and M. P. Sheetz. 1993. Force of single kinesin molecules measured with optical tweezers. *Science*. 260:232–234.
- Lawrence, M. B., and T. A. Springer. 1991. Leukocytes roll on a selectin at physiologic flow rates: distinction from and prerequisite for adhesion through integrins. *Cell*. 65:859–873.
- Lee, G. U., D. A. Kidwell, and R. J. Colton. 1994. Sensing discrete streptavidin-biotin interactions with atomic force microscopy. *Langmuir*. 10:354–357.
- Merkel, R., P. Nassoy, A. Leung, K. Ritchie, and E. Evans. 1999. Energy landscapes of receptor-ligand bonds explored with dynamic force spectroscopy. *Nature*. 397:50–53.
- Merkel, R., K. Ritchie, and E. Evans. 1995. Slow loading of biotin-streptavidin bonds yields unexpectedly low detachment forces. *Biophys. J.* 68:A404.
- Pierres, A., A. M. Benoliel, and P. Bongrand. 1995. Measuring the lifetime of bonds made between surface-linked molecules. *J. Biol. Chem.* 270: 26586–26592.
- Pierres, A., A. M. Benoliel, and P. Bongrand. 1998a. Studying receptor-mediated cell adhesion at the single molecule level. *Cell Adhesion Communication*. 5:375–395.
- Pierres, A., A. M. Benoliel, and P. Bongrand. 1998b. Use of a laminar flow chamber to study the rate of bond formation and dissociation between surface-bound adhesion molecules: effect of applied force and distance between surfaces. *Faraday Discuss.* 111:321–330.
- Pierres, A., A. M. Benoliel, P. Bongrand, and P. A. van der Merwe. 1996. Determination of the lifetime and force dependence of interactions of single bonds between surface-attached CD2 and CD48 adhesion molecules. *Proc. Natl. Acad. Sci. U.S.A.* 93:15114–15118.

- Pierres, A., A. M. Benoliel, C. Zhu, and P. Bongrand. 2001. Diffusion of microspheres in shear flow near a wall: use to measure binding rates between attached molecules. *Biophys. J.* 81:25–42.
- Pierres, A., H. Feracci, V. Delmas, A. M. Benoliel, J. P. Thiéry, and P. Bongrand. 1998. Experimental study of the interaction range and association rate of surface-attached cadherin 11. *Proc. Natl. Acad. Sci. U.S.A.* 95:9256–9261.
- Pierres, A., O. Tissot, B. Malissen, and P. Bongrand. 1994. Dynamic adhesion of CD8-positive cells to antibody-coated surfaces: the initial step is independent of microfilaments and intracellular domains of cell-binding molecules. *J. Cell Biol.* 125:945–953.
- Sano, T., and C. R. Cantor. 1995. Intersubunit contacts made by tryptophan 120 with biotin are essential for both strong biotin binding and biotin-induced tighter subunit association of streptavidin. *Proc. Natl. Acad. Sci. U.S.A.* 92:3180–3184.
- Snedecor, G. W., and W. G. Cochran. 1980. *Statistical Methods*. Iowa State University Press, Ames, Iowa.
- Stout, A. 2001. Detection and characterization of individual intermolecular bonds using optical tweezers. *Biophys. J.* 80:2976–2986.
- Tees, D. F., R. E. Waugh, and D. A. Hammer. 2001. A microcantilever device to assess the effect of force on the lifetime of selectin-carbohydrate bonds. *Biophys. J.* 80:668–682.
- Tha, S. P., J. Shuster, and H. L. Goldsmith. 1986. Interaction forces between red cells agglutinated by antibody. IV. Time and force dependence of break-up. *Biophys. J.* 50:1117–1126.
- Weber, P. C., D. H. Ohlendorf, J. J. Wendoloski, and F. R. Salemme. 1989. Structural origins of high-affinity biotin binding to streptavidin. *Science*. 243:85–88.
- Yuan, C., A. Chen, P. Kolb, and V. T. Moy. 2000. Energy landscape of streptavidin-biotin complexes measured by atomic force microscopy. *Biochemistry*. 39:10219–10223.